Tethering Functional Ligands onto Shell of Ultrasound Active Polymeric Microbubbles

Francesca Cavalieri, Ali El Hamassi, Ester Chiessi, and Gaio Paradossi*

Dipartimento di Scienze e Tecnologie Chimiche, Università di Roma Tor Vergata and INFM, 00173 Roma, Italy

Raffaella Villa and Nadia Zaffaroni

Istituto Nazionale per lo Studio e la Cura dei Tumori, 20133 Milano, Italy

Received September 28, 2005; Revised Manuscript Received November 29, 2005

Hollow (air-filled) microparticles, i.e., microbubbles, provide a promising novel vehicle for both local delivery of therapeutic agents and simultaneous diagnostic ultrasound echo investigations. In this paper, we describe the synthetic routes for decorating the polymeric shell of a poly(vinyl alcohol)-based microbubble with low and high molecular weight ligands with pharmacological relevance. Investigations on physical properties of microbubbles and surface chemical coupling with different cargo molecules such as L-cysteine, L-lysine, poly(L-lysine), chitosan, and β-cyclodextrin were carried out by CD and NMR spectroscopies, confocal laser scanning microscopy, and microcalorimetry. The in vitro cytotoxicity and biocompatibility of the polymer microbubbles have been also determined toward different cell lines. The results are discussed in terms of the features shown by this device, i.e., injectability, long shelf life, ease of preparation, biocompatibility, loading and cargo capacities, and functional properties.

Introduction

Microbubbles are nowadays a widely used diagnostic tool in contrast ultrasound imaging, and therapeutic use of these mesoscopic devices is a promising implementation in this field. Several types of microbubbles are commercially available as ultrasound enhancers for echographic investigations differing in their chemical nature.[1] Microbubbles based on air-filled denaturated albumin microcapsules, phospholipids, and liposomes containing gaseous SF_6 or perfluorocarbons have appeared to the market.[2]

In recent years, research work aimed at designing more efficient ultrasound contrast agents yielded important results demonstrated by new marketed products, but did not exhaust new and more demanding requirements that should be found in next-generation ultrasound imaging devices. One of the requisites sought in a multifunctional echographic contrast agent is to change the chemical properties of its surface to target an organ or a tissue.[3] In principle, this can be done by decorating the surface of the microbubbles with suitable hydrophilic and hydrophobic moieties functioning as selective targeting ligands increasing the affinity of the microbubble surface toward the tissues to be monitored.[4] Another important issue related to the multifunctionality of the microbubbles is the possibility of using such devices as drug delivery systems in different diseases including cancer.

A significant asset of microbubbles is their injectability compared to the oral administration of drugs suitable for tablets. In this way, the carrier, i.e., the microbubble, is able to arrive through the systemic circulation to the target organ and release the either chemically attached or encapsulated drug in situ by in-resonance ultrasonic irradiation and consequent bubble cavitation.

Surface modification of colloidal drug carriers dominates current strategies aimed at achieving such site-specific drug delivery.

Surface entrapment of bioactive molecules on poly(DL-lactide-*co*-glycolide) (PLGA) drug carrier microparticles was attempted by adding a functional surfactant or a polymeric emulsifier during production of the microparticles to carry DNA vaccines on the positively charged particle surface or to prolong the circulation time of the delivery vehicle.[5] Current approaches to enhance nonviral gene delivery involve the complexation of DNA with cationic liposomes[6] or polymers[7] such as poly(L-lysine) (PLL), poly(ethylenimine) (PEI),[8] or chitosan.[9] In this way, successful in vitro and in vivo transfections into mammalian cells were accomplished. However, the use of such assembled DNA complexes results in an internalization of approximately 20−50% of the added DNA, forbidding a prolonged in vivo usage. These drawbacks have stirred interest for the development of alternative delivery modalities and devices. A working hypothesis to circumvent such difficulties is to immobilize DNA in a biomaterial scaffold to fulfill the requirements of safe gene vector circulation in vivo and of controlling the prolonged release of genetic material at constant concentration with a defined time pattern: ultrasound active microbubbles can represent a promising device as vectors for gene delivery. Following this idea, plasmid DNA was loaded on the albumin microbubble shell during the synthesis, enhancing the ultrasound gene transfection and gene expression in vitro.[10] In vivo developments of this approach may represent an improved avenue for therapeutic gene delivery. Incorporation of DNA or other therapeutic agents into the shell of the microbubbles may exert several important functions: drug or plasmid DNA will be present at high concentration and protected from circulating DNAses at the site of microbubble destruction. Moreover, the inertial cavitation of microbubbles may facilitate transvascular delivery or intracellular deposition of therapeutic

* Corresponding author email address: paradossi@stc.uniroma2.it.

10.1021/bm050723g CCC: $33.50
Published on Web 01/19/2006

Table 1. Ideal Microbubble Properties for Diagnostic and Therapeutic Purposes

functional property	structural property
injectability	average external diameter $\geq 5\ \mu$m narrow size distribution
ultrasound scattering efficiency	highest density and compressibility difference between medium and microbubbles
biocompatibility	suitable surface chemical moieties
drug payload	suitable reactive chemical functionalities at the surface
drug delivery	inertial cavitation in biomedical working frequency range: 1−4 MHz suitable mechanical properties of the shell and shell thickness narrow thickness distribution

agents. In pursuing this approach, we were able to produce aqueous suspensions of air-filled polymer microbubbles with limited size polydispersity obtained with a method that differs from those described in the literature.[11−13] In our case, air was entrapped in a polymer shell obtained by chemically cross-linking modified poly(vinyl alcohol) (PVA) at the air−water interface. The PVA-based microbubbles were separated by flotation and stocked as a water suspension, showing a shelf life of many months. Considering the interaction of microbubbles with ultrasound, the formulation of a class of mesoscopic systems functioning simultaneously as echo-contrast and drug delivery agents can be assessed. The echogenic properties, in terms of the pressure threshold at which these microbubbles undergo inertial cavitation, are under investigation, and preliminary studies on in vitro biocompatibility of PVA microbubble formulation encouraged our research. Therefore, the ultimate goal of our work is to develop drug-loaded PVA microbubbles that can be conveyed by implantable microfluidic components such as micropumps, with the ability to store and locally release drug carriers in response to external stimuli such as ultrasound. Ideal injectable polymeric microbubbles should feature the properties listed in Table 1.

Recently, we described the synthesis and physical properties of PVA-based microbubbles derived from interfacial cross-linking of telechelic PVA via acetalization.[12,13] These PVA-based microbubbles offer the possibility of tuning the loading and release of high and low molecular weight drug compounds tailoring the microbubble surface chemical properties and methods of functionalization. Moreover, there is a wide variety of covalent attachment procedures for functionalizing our PVA-coated microballoons. We anchored several bioactive molecules ranging from oligopeptides, amino acids, and oligosaccharides to polysaccharides. These molecules were sorted out according to their potential pharmacoactivity as follows.

- β-Cyclodextrin modified microbubbles can be used to include and deliver lipophilic drugs.
- Cationic polymers as poly(L-lysine) and chitosan can self-assemble DNA to form a complex tethered to the surface of the microbubbles. In this respect, this system can be regarded as a model for potential uses in gene therapy.

Experimental Section

Materials. Poly(vinyl alcohol) was a Sigma product. Number average molecular weight determined by membrane osmometry was 30 000 ± 5000 g/mol, and weight average molecular weight of 70 000 ± 10 000 g/mol was determined by static light scattering.

Chitosan with number average molecular weight of 50 000 ± 5000 g/mol and degree of acetylation of 0.1 was purchased from Sigma. L-Lysine HCl, L-cysteine HCl, β-cyclodextrin, amantadine, poly(L-lysine) HBr (PLL) with a molecular weight of 7500 g/mol, and 5,5′-dithio-bis(2-nitrobenzoic acid) (DTNB) were purchased from Sigma and used without further purification. Potassium pectate, i.e., poly(D-galacturonate) potassium salt, obtained from citrus pectin after complete de-esterification[14] was a kind gift of Dr. A. Malovikova, Slovak Academy of Science, Bratislava. The D-galacturonate content of pectate was 90.3%, and a number average molecular weigth of 19 000 g/mol was determined by membrane osmometry. Fluorescein isothiocyanate isomer I, FITC, rhodamine B isothiocyanate, RBITC, and 5-(4,6-dichlorotriazinyl)aminofluorescein, DTAF, were Fluka products. All inorganic chemicals were reagent grade from Carlo Erba. Water was Milli-Q purity grade (18.2 MΩ·cm), produced with a deionization apparatus (PureLab) from USF.

Dialysis membranes with a cutoff of 12 000−13 000 daltons were purchased from Medicell, Italy.

Methods. *Synthesis of PVA-Coated Microbubbles.* Synthesis of telechelic PVA was previously described in the literature.[11−12] Stable (air-filled) PVA-coated microbubbles were prepared by cross-linking telechelic PVA at the water/air interface. Vigorous stirring at room temperature for 3 h of 2% telechelic PVA aqueous solution (100 mL) at pH 2.50 by an Ultra-Turrax T-25 at 8000 rpm equipped with a Teflon-coated tip generated a fine foam of telechelic PVA acting both as colloidal stabilizer and as air bubble coating agent. The cross-linking reaction was carried out at room temperature and at 5 °C by adding hydrochloric or sulfuric acid as catalyst and stopped by neutralizing the mixture. Floating microbubbles were separated from solid debris and extensively dialyzed against Milli-Q water. The aqueous suspensions of microbubbles were obtained and used for further chemical modification.

Preparation of β-Cyclodextrin Functionalized Microbubbles. Covalent linkage of β-cyclodextrin to microbubbles was achieved by acetalization reaction between microbubble suspension (1 mg/mL) and a 0.02 M β-cyclodextrin aqueous solution. After incubation for 24 h at 25 °C and pH 3, the resulting mixture was neutralized and extensively dialyzed against water in order to remove free β-cyclodextrin.

Preparation of L-Lysine Functionalized Microbubbles. PVA chain end segments on a microballoon shell were end capped with L-lysine via Schiff base linkages. The microbubble suspension (1 g/L) was incubated with 0.7 g/mL solution of lysine at 25 °C, and pH was adjusted to the optimal value of 5.0. After 48 h, microbubbles were dialyzed against water to remove unreacted amino acid.

Preparation of L-Cysteine Functionalized Microbubbles. Covalent linkage of L-cysteine to microbubbles was achieved by the reductive amination procedure. A 10 mL sample of aqueous suspension of microbubbles (2 mg/mL) was incubated with 0.5 M cysteine aqueous solution at 25 °C at pH 5. Schiff base reduction was carried out by $NaBH_3CN$. After 5 days, microbubbles were extensively dialyzed to remove unreacted amino acid.

Preparation of Poly(L-lysine) Functionalized Microbubbles. Poly(L-lysine), PLL, was linked to microbubbles by imine linkages or by the reductive amination procedure. A 10 mL sample of aqueous suspension of microbubbles (1 mg/mL) was incubated with 3 g/L solution of poly(L-lysine) (M_w 7500) at room temperature and pH 5. Schiff base reduction was carried out by $NaBH_3CN$. After 48 h, microbubbles were extensively dialyzed to remove unreacted poly(L-lysine). A dialyzed suspension of poly(L-lysine) coupled to microbubbles was concentrated by recovering the floating microparticles and used for spectroscopic investigations. PLL−poly(D-galacturonate) complexes were prepared by mixing at pH 6 in a 1:1 charge ratio potassium poly(D-galacturonate) (M_n 19 000) with poly(L-lysine).

Preparation of Chitosan Functionalized Microbubbles. Chitosan was conjugated to microbubbles by using the reductive amination procedure. Chitosan was dissolved in sodium acetate 0.2 M acetic acid 0.3 M buffer at pH 4.5 to a concentration of 3.3% (w/v). A 5 mL sample of

2 mg/mL microbubble aqueous suspension was added with 0.8 mL of chitosan solution at room temperature. The pH was carefully adjusted to 5.0 with acetate buffer, following the addition of $Na(CN)BH_3$. The resulting suspension was stirred for 5 days at room temperature. The microbubble suspension was then extensively dialyzed and washed to remove unreacted chitosan.

Characterization of Unmodified and Derivatized PVA Microbubbles. Particle size distribution was evaluated by dynamic light scattering (DLS), matching the density of the particles to that of the medium. An 80/20 water/acetone mixture was used as density matching liquid. For these measurements, a BI-200SM goniometer (Brookhaven Instrument Co.), equipped with a diode pumped solid-state laser (Suwtech) at 532 nm was used. The correlation functions were analyzed according to the CONTIN algorithm.

FITC and RBITC were used for fluorescent labeling of the microbubbles. Fluorescent dyes were added into the suspension at a typical concentration of 10 μM. Floating particles were washed by resuspending them in Milli-Q water several times. Confocal images were collected by a confocal laser scanning microscope (CLSM), Nikon PCM 2000 (Nikon Instruments; a compact laser scanning microscope based on a galvanometer point-scanning mechanism), a single pinhole optical path, and a multi-excitation module equipped with Spectra Physics Ar ion laser (488 nm) and He−Ne laser (543.5 nm) sources. A 60×/1.4 oil immersion objective was used for the observations. Tests carried out by measuring giant liposome shells provided a value of 0.25 μm for instrumental resolution. Shell thicknesses of fluorescent-labeled microparticles were measured as the full width at half-maximum of the fluorescence intensity profile.

Circular dichroism (CD) spectra typically in the range 210−300 nm were recorded by using a quartz cell (1−10 mm) with JASCO J600 spectrometer equipped with a thermoregulated cell compartment to check the microbubble surface modification by L-lysine, L-cysteine, and poly(L-lysine) and to observe peptide conformational behavior as a function of pH and in the presence of poly(D-galacturonate). The aqueous microbubble suspension (1 mg/mL) was only slightly turbid, and the CD spectrum was recorded using an untreated microbubble suspension as a blank to determine the absence of artifacts in the CD spectrum. Only after this check was a quantitative estimation of bound poly(L-lysine) concentration attempted.

The CD spectrum of the PLL−poly(D-galacturonate) complex assembled on microbubbles was recorded on a mixture of the negatively charged polysaccharide and PLL loaded microbubbles at the molar ratio of 1:1.[14]

High-resolution ^1H NMR spectra were recorded on a Bruker 400 MHz on a D_2O suspension of microbubbles to check the conjugation of L-cysteine and β-cyclodextrin to the microbubble surface. The thiol content introduced on the microbubbles by functionalization with L-cysteine was determined using Ellman's reagent.

Isothermal microcalorimetry titration of β-cyclodextrin anchored microbubbles with amantadine hydrochloride allowed the determination of both the extent of microbubble grafting and the binding constant of the inclusion complex. Binding constant determination of the free β-cyclodextrin−amantadine complex in solution was carried out as well. Binding measurements were carried out with an isothermal microcalorimeter, TAM (Thermometrics), at 25 °C by adding 10 μL of amantadine solution (0.015 M) to 2 mL of concentrated microbubble aqueous suspension placed in a stainless cell. Potentiometric titration of glucosamine residues of chitosan was used for quantitative estimation of chitosan conjugation to microbubbles.

Cell Lines and Cell Growth Assay. LoVo and HT29 human colon adenocarcinoma cell lines obtained from American Type Culture Collection were used for cytotoxicity tests. According to growth profiles preliminarily defined for each cell model, appropriate numbers of cells in the logarithmic growth phase were plated in each well of a 6-well plate and allowed to attach to the plastic surface for 24 h. Cells were then exposed to increasing volumes of 1 g/L PVA microbubble suspensions for 7 days at 37 °C in a 5% CO_2 humidified atmosphere in air. At the end of incubation, cells were counted in a particle counter (Coulter Counter, Coulter Electronics, Luton, U.K.). Each experimental point was run in triplicate.

Chart 1. Schematic Representation of the Air-Polymer Shell-Water Boundary

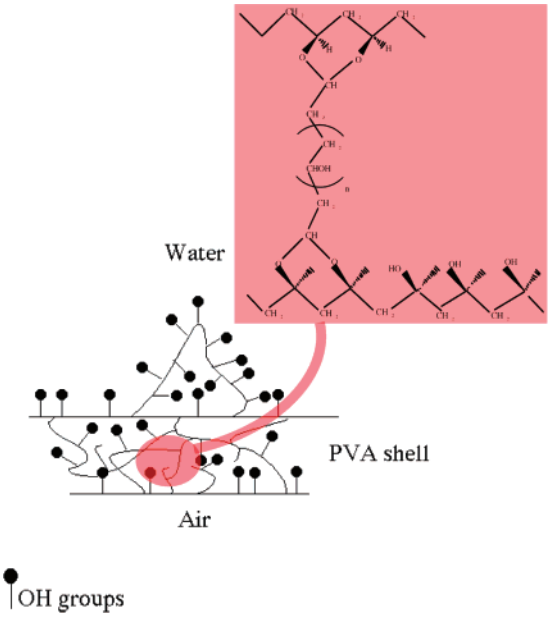

Results and Discussion

Characterization of the Microbubbles. We have already described in a previous work[13] the synthetic route of polymeric microballoons by carrying out a cross-linking reaction of a telechelic PVA, i.e., a PVA bearing aldehydes at the chain ends, at the air/water interface. Factors leading to the formation of microbubbles coated by a PVA shell have also been pointed out. In Chart 1, the shell microbubble structure is depicted at the air and water boundary.

Acetalization of telechelic PVA at the air−water interface under high shear condition leads to the formation of spherical polymer shells entrapping air in the micron-sized particle core. Separation of these particles, characterized by a density lower than water, from PVA debris is particularly easy because of the flotation of the empty microspheres toward the surface of the aqueous suspension. In the early stage of the polymer shell formation, the PVA surfactant behavior causes migration of chains at the air/water interface. The initial polymer layer will assume a spherical shape with dimensions dictated by the Laplace equation. Accumulation of PVA molecules will occur according to the Gibbs adsorption equation up to the leveling off of the surface tension with PVA concentration.[15] Simultaneously, the acetalization process supplies the necessary chemical cross-links to stabilize the shell of particles. PVA permeability to gases and particularly to nitrogen is very low, thus offering a barrier against air escape. The air-filled microbubble aqueous suspensions display a shelf life of many months. Colloidal stabilization of such a system caused by the presence of polymer chains protruding into the bulk medium prevents particle coagulation.

The yield of polymer microbubble fabrication drastically depends on several experimental parameters, and the choice of proper operative conditions is a key point for performing successful microbubble design. The influence of reaction parameters such as telechelic PVA concentration, acid catalyst

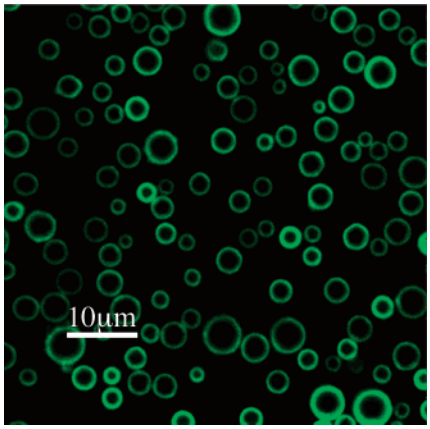

Figure 1. 2D CLSM image of FITC-labeled PVA-based microbubbles.

Table 2. Structural Parameters of PVA Microbubbles

external diameter μm	internal diameter μm	shell thickness μm	specific surface area m^2/g
$5^a \pm 1$	$3^a \pm 1$	$0.90^a \pm 0.25^c$	1.2
$5^b \pm 1$			

[a] Confocal laser scanning microscopy. [b] Dynamic light scattering. [c] Confocal microscope resolution.

concentration, time of reaction, and reaction temperature on the preparation of microbubbles[13] were scrutinized in detail. The use of 2% (w/w) fully hydrolyzed telechelic PVA, 0.02 M H_2SO_4 as catalyst, and stirring for 3 h at 5 °C resulted in the higher microparticle density of $7 \cdot 10^7$ microbubbles/mL. The CLSM image in Figure 1 shows a typical PVA-based microbubble preparation.

The structural characterization of microballoons prepared at room temperature was studied by CLSM. FITC labeling was used to visualize the shells and to determine microparticle size and shell thickness (see Table 2).

Polydispersity of the microbubble external diameter was determined by dynamic light scattering evaluation of the autocorrelation function by the CONTIN method, operating in a mixed solvent (water/acetone 80:20) in order to minimize the interference of buoyancy of the microbubbles on the correlation function. As mentioned above, we have observed a remarkably long shelf life of the aqueous suspension of these systems, a feature often claimed as a prerequisite for ultrasound imaging

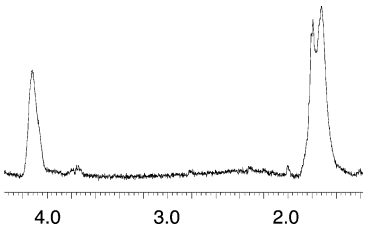

Figure 2. ^1H NMR spectrum of D_2O microbubble suspension.

devices. However, most of the commercially available products match these requirements only partially. In this context, the chemical and physical stability of these air-filled microbubbles based on the use of a biocompatible polymer represent an asset for considering this system as a potential ultrasound echo contrast and drug delivery tool.

To address the device to the targeted organ and promote focal release of the drug payload, suitable functionalization of the polymeric shell has to be devised. We have probed the possibility of covalently anchoring different types of case molecules to the microbubble external surface: L-lysine, L-cysteine, β-cyclodextrin, poly(L-lysine), and chitosan. The chemical functionalization of microbubbles described in this work is summarized in Chart 2. The attachment route is mostly determined by the chemical nature of the microbubble polymer shell. Microbubble surface reactivity is an important parameter for the functionalization and loading capacity. However, this feature could be detrimental to the biocompatibility properties of the microbubbles. In our case, shell formation entails intermolecular acetalization. Few unreacted chain ends bearing aldehyde groups at physiological pH are in the form of intramolecular stable hemiacetal tethered to the shell and protruding toward the solution. These chain ends can be activated at acidic pH, offering simple routes to conjugated molecules carrying hydroxyl or amino moieties by acetalization or Schiff base coupling, respectively.

The ^1H NMR spectrum in Figure 2 of a microbubble suspension in D_2O indicates high flexibility of PVA chains, as rather sharp signals were recorded for PVA backbone methine and methylene groups at 4.1 and 1.5 ppm, respectively. These polymer chain tentacles, protruding toward the solution from the microbubble surface, exhibit a mobility similar to that measured in solution, whereas the polymer chains engaged in the buildup of the shell have a much lower mobility, and their relaxation decays are silent to the probed NMR time scale.

Chart 2. Scheme of Microbubble Chemical Functionalization (structures not in scale)

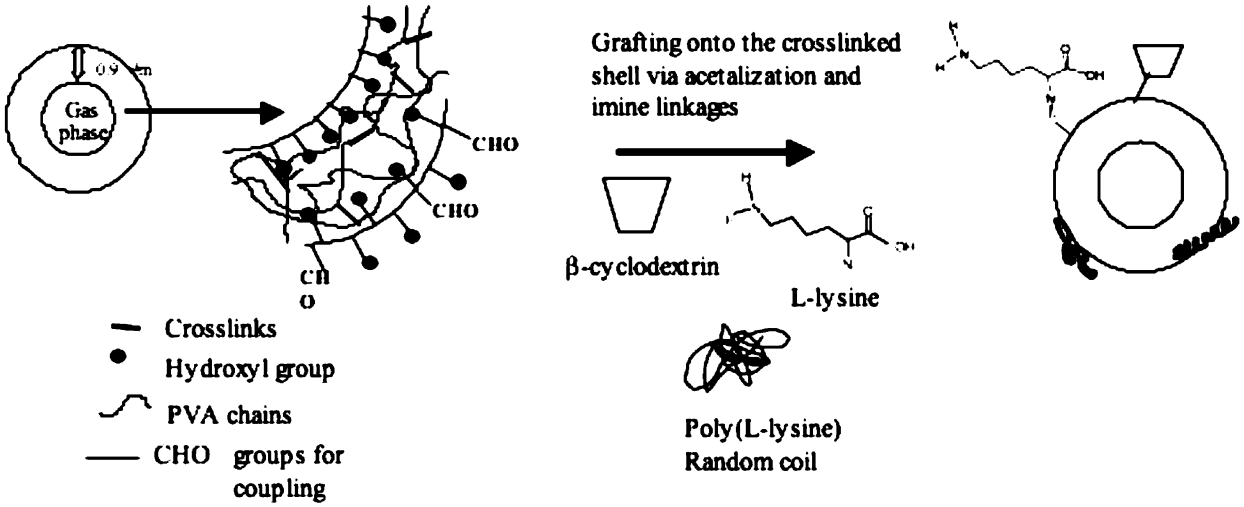

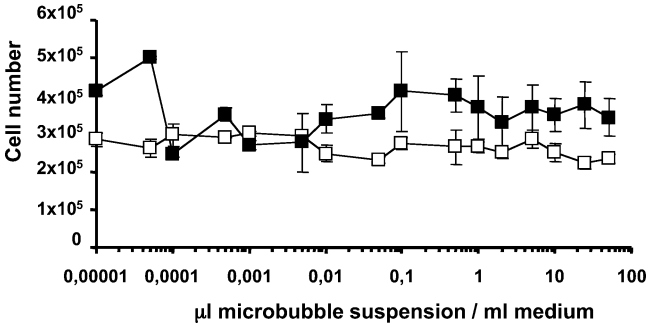

Figure 3. Growth of human colon adenocarcinoma cell lines, LoVo (■) and HT29 (□), exposed to different volumes (from 0 to 50 μL/mL culture medium) of PVA microbubbles after 7 days. Data represent mean values (±SD) of three independent experiments.

The presence of masked aldehydes in the form of intramolecular hemiacetals at physiological pH is a central factor for the biocompatibility of the microbubbles towards several cellular strains, as reactive aldehyde groups on microbubbles are known to be highly cytotoxic.

Colon adenocarcinoma cell lines were chosen for biocompatibility tests for two main reasons: (i) the related malignancy represents one of the most common human tumor types, and (ii) it is largely refractory to current anticancer therapies and could benefit from the development of new strategies based on innovative delivery systems for conventional anticancer drugs as well as on gene therapy approaches. We evaluated the effect of long-term (7 day) exposure to increasing concentration of PVA microbubbles on the in vitro cell growth of two human colon adenocarcinoma cell lines, LoVo and HT29, as shown in Figure 3. No significant antiproliferative effect was observed in cells exposed to microbubbles compared to control cells in both experimental models, indicating that microbubbles do not leach any cytotoxic fragment.

The evaluation of the effect of long-term (7 day) exposure to increasing concentrations of PLL-coated microbubbles resulted in a negligible interference with LoVo cell growth at concentrations up to 20 μg/mL. Higher concentrations induced an appreciable and dose-dependent decline of LoVo proliferation. However, short-term (1 day) exposure to different concentrations of PLL-coated microbubbles failed to affect LoVo cell growth at all tested concentrations (from 5 to 200 μg/mL).

Moreover, when examined under a phase-contrast microscope, cells showed comparable morphology and shape with respect to control cells (not shown). These findings indicate that PVA microbubbles do not interfere with tumor cell growth and can be considered a biocompatible support for the development of new drug delivery systems.

Chemical reactivity of the microbubble surface was tested by using both low and high molecular weight molecules. For the former type of molecules, the extent of functionalization was qualitatively assessed by spectroscopic methods, whereas for β-cyclodextrin, PLL, and chitosan modified microbubbles, a quantitative evaluation of derivatization was assessed.

L-Lysine and L-Cysteine Microbubble Surface Functionalization. Microbubbles bearing pendant aldehyde groups were designed to react with amino acids via imine linkage formation under very mild condition.

L-Lysine can be attached to the particle surface by Schiff base coupling at the α- or ϵ-amino group positions, the former group being much more reactive (pK_a 8).

The CD spectrum of a L-lysine grafted microbubble suspension is shown in Figure 4. Comparison with the CD spectrum of the original amino acid shows that the ellipticity of the lysine

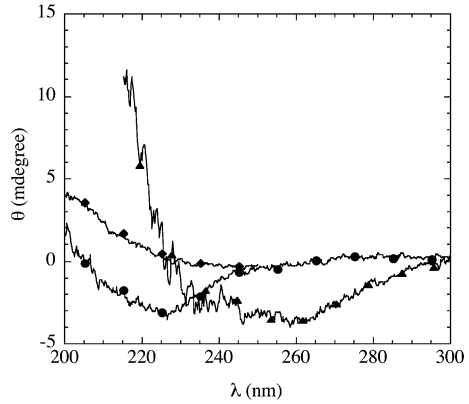

Figure 4. Room-temperature CD spectra of lysine aqueous solution 1.6 10^{-3} M at pH 6 (0.1 cm cell) (◆), lysine modified microbubble suspension (1 mg/mL, 0.1 cm cell) (●), cysteine modified microbubble suspension (1 mg/mL, 1 cm cell) (▲).

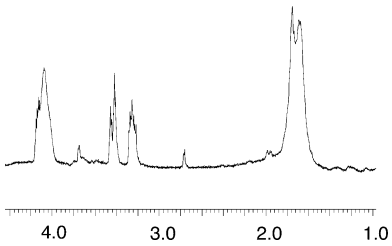

Figure 5. ^{1}H NMR spectrum of D_2O suspension of L-cysteine modified microbubbles.

modified microbubbles presents a remarkable change in the sign. The negative CD band indicates that the lysine coupling involves mainly the more reactive α-amino groups, changing the Cotton effect sign intensity associated with the n → π^* transition of the carboxyl groups.

PVA microbubbles were modified by cysteine to introduce disulfide and thiol moieties on their surfaces. The CD spectrum of cysteine coupled microbubbles, reported in Figure 4, was recorded in order to qualitatively check the successful conjugation to the microbubbles surface. Disulfide bonds give rise to a diagnostic broad signal throughout the near-UV CD spectral region, indicating that a simple oxidation process in aqueous media leads to the formation of inter- and/or intrachain disulfide bonds within the thiolated surface microbubbles. As a quantitative evaluation of cysteine/cystine content was not accessible by CD, thiol content on the microbubbles determined using Ellman's reagent was 4.8 meq/mg. The presence of cysteine on the microbubble surface was also evidenced by the high-resolution NMR spectrum recorded on the D_2O microbubble suspension (Figure 5), displaying resonance peaks of the methylene group of the cysteine moiety at 3.2−3.4 ppm.

Thiols carrying polymeric microparticles were recently developed as an in vitro protein refolding device mimicking the function of the molecular chaperones.[16] Polymeric microbubbles carrying thiol and disulfide groups are able to bind and refold reduced proteins via thiol−disulfide exchange reaction. Moreover, thiolated microbubbles strongly improve the mucoadhesive properties of a drug delivery system, ensuring localization of the drug at a given target site.[17]

Poly(L-lysine) Surface Microbubbles Decoration. Modern therapeutic approaches use macromolecular assemblies to penetrate cellular membranes and ultimately introduce gene sequences.[6,7,18] DNA recognition by helical peptides containing lysine residues by the formation of a macromolecular complex

with the capability to be endocytosed by cells has been reported in the literature.[8,9,19]

In this respect, we have tested the possibility of decorating the external surface of PVA-based microbubbles with poly(L-lysine), PLL, and investigated the conformational properties of the anchored polypeptide. PLL conjugation on a polymeric shell was carried out by Schiff base formation using the presence of the acetal moiety on the microbubble shell and of the amino groups of poly(L-lysine). The total amount of tethered polypeptide was 81 mg lysine residue/g microbubbles corresponding to 67 mg/m^2, based on a specific surface area of microbubbles of 1.2 m^2/g (see Table 1) and molar ellipticity of PLL in random coil conformation measured by circular dichroism. Reductive amination of the Schiff bases increases the PLL amount on the microbubble surface to about 550 mg/m^2. These payloads are higher than the protein and PLL contents, evaluated in about 1 to 3 mg/m^2, obtained at the oil/water interfaces[20] and at the PLGA surface microparticles,[5] respectively.

Moreover, the chemical stability of the poly(L-lysine) tethered microbubbles was greatly improved by the reductive amination step. Tethered PLL by Schiff base conjugation was hydrolyzed in few weeks, whereas the reductive amination yielded an amine linkage resulting in a product stable for few months.

The conformational properties of poly(L-lysine) immobilized on the microbubble shell were investigated in order to understand the potential of these devices as carriers able to retain the conformational status of the attached macromolecule. The ability of polypeptides to undergo an α-helix ↔ random coil transition by varying the solution parameters such as pH, temperature, and solvent polarity is known.[21] The conformational features of PLL anchored to PVA-based microbubbles were tested by circular dichroism spectroscopy, an assessed approach for investigating the conformational state of polypeptides. The α-helix content of the polypeptide was evaluated by the method of Greenfield and Fasman.[21] With the α-helix content of the low molecular weight PLL set to 100%, about 72% of the polypeptide anchored as Schiff base or as amine was in the ordered conformation, according to the analysis of the CD spectrum of a suspension of PLL-decorated microbubbles shown in Figure 6a.

Another check on the conformational properties of the anchored polypeptide was carried out by studying the interaction of tethered PLL with the oppositely charged poly(D-galacturonate). Recently, we investigated[14,22] the conformation in aqueous solution of the macromolecular complex between PLL and poly(D-galacturonate). It has been established that the interaction between these oppositely charged polyelectrolytes induces the formation of an ordered assembly constituted by an α-helical conformation of the peptide and a super-helical arrangement of the polysaccharide moiety. The influence of the anchoring on the conformational status of the polypeptide in the presence of the polysaccharide moiety is shown in Figure 6b. In this case, the ordered conformation of immobilized PLL on the microbubble surfaces approaches 40% with respect to the molar ellipticity of the corresponding low molecular weight PLL at basic pH. To avoid the poly(D-galacturonate) ellipticity contribution in the region of 220−200 nm, the observed spectrum was "best fitted" only between 250 and 230 nm for the determination of the α-helix content in PLL. It should be considered that polyelectrolyte complexes typically have a low solubility in water, whereas the high PLL total surface entrapment obtained by reductive amination indicates that surface immobilization represents an efficient method to carry a higher concentration of supramolecular complex.

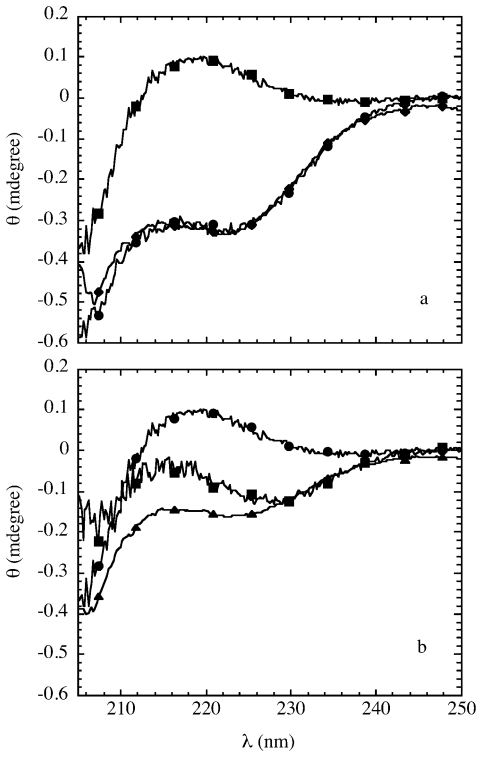

Figure 6. (a) Room-temperature CD spectra of poly(L-lysine) anchored on PVA microbubbles via reductive amination: pH 12 (●); pH 7 (■); full line simulation at pH 12 (◆). (b) Room-temperature CD spectra of 1:1 anchored poly(L-lysine)−poly(D-galacturonate) mixture, 0.0018 M (■) on microbubble surface; random coil of anchored PLL to microbubble surface at pH 7 (●); simulation of CD curve in the range 250−200 nm (▲).

Some considerations can be inferred on the conjugation site of poly(L-lysine). Both ϵ- and terminal α-amino groups, present in this peptide, can participate in the anchoring of the peptide molecule. In our case, the number of amino groups in the ϵ-position is about 40 times the number of the α-amino group. However, the terminal amino groups possess a higher reactivity. The conservation of the conformational features of the tethered poly(L-lysine) indicates that the conjugation sites are most probably the α-amino groups, as the involvement of amino groups of the ϵ-type would dramatically decrease the ability of peptide chains to undergo a conformational transition in the observed extent. Moreover, α-amino groups coupling to the microbubble surface preclude interbubble bridging processes, as the remaining ϵ-type ones have a much lower reactivity.

Figure 7 shows that tethered PLL promotes microbubble aggregation at basic pH. As already described in the literature,[5] in these conditions the polypeptide is neutral, and hydrophobic effects drive the behavior of this colloidal system. The lowering of pH promotes aggregate disruption, confirming that PLL is not able to chemically link microbubbles.

***β*-Cyclodextrin Surface Decoration.** Liposoluble drugs can be effectively incorporated in the lipid layers of vesicle-type microbubbles.[4] Also, the β-cyclodextrin hydrophobic cavity can be exploited to accommodate lipophilic molecules.[23] The acetalization reaction can be used to couple the carbonyl end groups of the telechelic PVA chains projecting from the microbubble surface in the solution and the hydroxyl moiety of β-cyclodextrins. In Figure 8, the ^{1}H NMR spectrum in the 3.4−4.0 region indicates the microbubble surface derivatization with β-cyclodextrins.

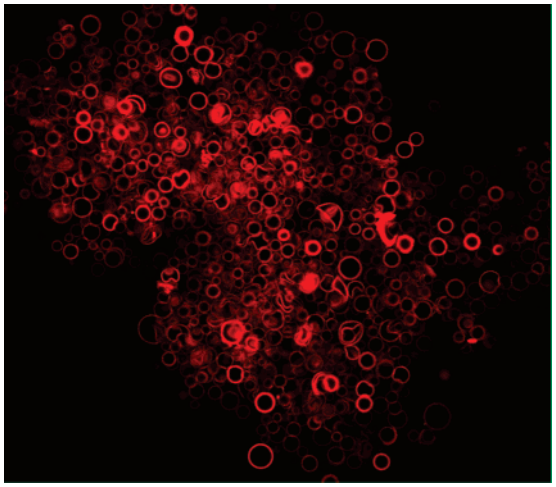

Figure 7. CLSM of an aqueous suspension of microbubbles with tethered PLL at pH 10.

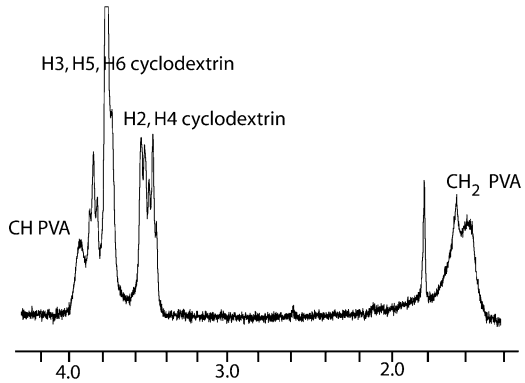

Figure 8. Proton NMR spectrum of derivatized PVA microbubbles with β-cyclodextrin.

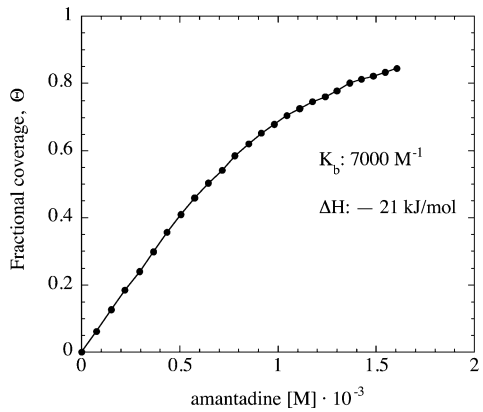

Figure 9. Binding isotherm of amantadine to microbubble anchored β-cyclodextrin at room temperature; continuous line nonlinear best fit.

The sharpness of peak resonances of β-cyclodextrins and PVA protons denotes a mobility comparable with the solution spectra of the two separate moieties.

In modeling the transport of a drug molecule, the inclusion capability of anchored β-cyclodextrins was studied by isothermal microcalorimetric titrations with amantadine, a molecule with known hydrophobic features.

An apparent binding constant of 7000 M^{-1} was determined by a nonlinear two-parameter fit of the data[24] assuming a 1:1 host/guest stoichiometry (Figure 9). The concentration of β-cyclodextrins host molecule effectively anchored on the microbubble surface was equal to 1 mM, corresponding to a ratio of 3.5 mol % β-cyclodextrin per mol PVA, with a binding enthalpy of -21 kJ/mol.

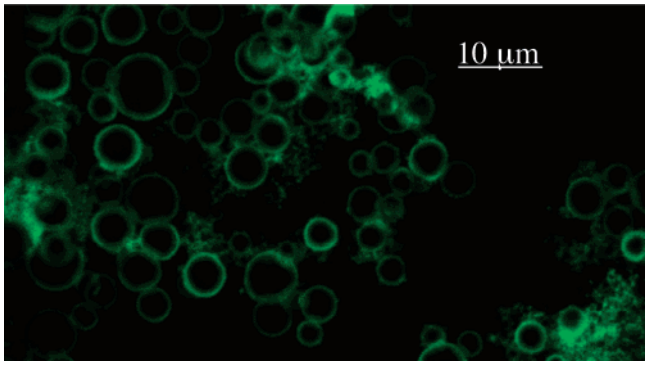

Figure 10. CLSM of chitosan-coated microbubbles.

Similar binding parameters, i.e., $K_b = 9000\ M^{-1}$ $\Delta H = -16$ kJ/mol, were determined for the β-cyclodextrin−amantadine complex in solution, thus showing that the anchoring did not change the inclusion properties of β-cyclodextrins.

Chitosan Surface Microbubbles Decoration (Figure 10). Chitosan has the special feature of adhering to mucosal surfaces and improving the bioadhesion.[25] For this reason, a variety of chitosan-based colloidal delivery carriers have been described for association and delivery of macromolecular compounds such as peptides, oligonucleotides, and genes. Because of the high molecular weight of chitosan, the extent of polysaccharides covalently bound to microbubbles, determined by potentiometric titration of microbubbles suspension, was very high, approximately 20 g % glucosamine/g microbubbles. The high yields of functionalization were also confirmed by confocal microscopy images where chitosan aggregates surrounding microbubbles were also evidenced by FITC labeling. As for PLL, protonation of amino groups discourages microbubble aggregation, indicating that covalent cross-linking is unlikely.

Concluding Remarks

PVA-based microbubbles offer interesting features as potential drug delivery devices. The unusual chemical and colloidal stability of these polymer microbubbles is the result of many factors such as the covalent nature of the cross-links responsible for the shell buildup and the presence of chain segments projecting into the dispersion medium with "good solvent" characteristics.

The combination of their properties as ultrasound enhancers with the ease in derivatizing their surface provides a clue for a new multifunctional ultrasound device with high chemical and physical stability. We have reported the conjugation of several pharmacologically relevant molecules to the surface of these microbubbles, addressing the characteristics of the system in targeting a tissue by increasing its bioadhesion properties, delivering by sonoporation the macromolecular cargo in the cell.

PLL and β-cyclodextrin coated microbubbles display interesting features as preservation of the typical random coil to α-helix conformational transition and of the ability to host molecules with hydrophobic features.

Such devices, showing good biocompatibility and physical stability, can be envisaged as an ultrasound responsive biomedical device.

Acknowledgment. We acknowledge partial support for this work from the INFM FIRB grant RBNE01XPYH and GEMI foundation 2005 grant.

CDV

References and Notes

(1) Schutt, E. G.; Klein, D. H.; Mattrey, R. M.; Riess, J. G. *Angew. Chem., Int. Ed.* **2003**, *42*, 3218−3235.
(2) Feinstein, S. B. *Am. J. Physiol.: Heart Circ. Physiol.* **2004**, *287*, H450−H457.
(3) Lindner, J. R. *Am. J. Cardiol.* **2002**, *90*, 72J−80J.
(4) Unger, E. C.; Porter, T.; Culp, W.; Labell, R.; Matsinaga, T.; Zutshi, R. *Adv. Drug Deliv. Rev.* **2004**, *56*, 1291−1314.
(5) Cui, C.; Schwendeman, S. P. *Macromolecules* **2001**, *34*, 8426−8433.
(6) Lee, G.; Schaffer, D. *Somatic Cell. Mol. Genet.* **2002**, *27*, 17−25.
(7) Ogris, M.; Wagner, E. *Somatic Cell. Mol. Genet.* **2002**, *27*, 85−94.
(8) Segura, T.; Volk, M. J.; Shea, L. D. *J. Controlled Release* **2003**, *93*, 69−84.
(9) Liu, W.; Sun, S.; Cao, Z.; Zhang, X.; Yao, K.; Lu, W. W.; Luk, K. D. K. *Biomaterials* **2005**, *26*, *2705*-2711.
(10) Frenkel, P. A.; Chen, S.; Thai, T.; Shohet, R. V.; Grayburn, P. A. *Ultrasound Med. Biol.* **2002**, *28*, 817−822.
(11) Paradossi, G.; Cavalieri, F.; Chiessi, E.; Spagnoli, C.; Cowman, M. K. *J. Mater. Sci.: Mater. Med.* **2003**, *14*, 687−691.
(12) Paradossi, G.; Cavalieri, F.; Chiessi, E.; Ponassi, V.; Martorana, V. *Biomacromolecules* **2002**, *3*, 1255−1262.
(13) Cavalieri, F.; El Hamassi, A.; Chiessi, E.; Paradossi, G. *Langmuir* **2005**, *21*, 8758−8764.
(14) Paradossi, G.; Chiessi, E.; Malovikova, A. *Macromolecules* **2001**, *34*, 8179−8186.
(15) Bhattacharya, A.; Ray, P. J. *J. Appl. Polym. Sci.* **2004**, *93*, 122−130.
(16) Shimizu, H.; Fujimoto, K.; Kawagichi, H. *Biotechnol. Prog.* **2000**, *16*, 248−253.
(17) Marscutz, M. K.; Bernkop-Schnürch, A. *Eur. J. Pharm. Sci.* **2002**, *15*, 387−394.
(18) Ochiya, T.; Nagahara, S.; Sano, A.; Itoh, H.; Terada, M. *Curr. Gene Therapy* **2001**, *1*, 1−13.
(19) Toncheva, V.; Wolfert, M. A.; Dash, P. R.; Oupicky, D.; Ulbrich, K.; Seymour, L. W.; Shacht, E. H. *Biochem. Biophys. Acta* **1998**, *1380*, 354−368.
(20) Dickinson, E. *J. Chem. Soc., Faraday Trans.* **1992**, *88*, 2973−2983.
(21) Greenfiled, N.; Fasman, G. D. *Biochemistry* **1969**, *8*, 4108−4115.
(22) Paradossi, G.; Chiessi, E.; Malovikova, A. *Biopolymers* **1999**, *20*, 201−209.
(23) Thorsteinn, L.; Mar, M. *Int. J. Pharm.* **2001**, *225*, 15−30.
(24) Paradossi, G.; Cavalieri, F.; Chiessi, E. *Macromolecules* **2002**, 35, 6404−6411.
(25) Janes, K. A.; Calvo, P.; Alonso, M. J. *Adv. Drug Deliv. Rev.* **2001**, *47*, 83−97.

BM050723G